

An overview of synthetic-type control charts: Techniques and methodology

Athanasios C. Rakitzis¹, Subhabrata Chakraborti^{2,3,*}, Sandile C. Shongwe³, Marien A. Graham⁴,
Michael Boon Chong Khoo⁵

¹Department of Statistics and Actuarial- Financial Mathematics, University of Aegean, Karlovasi, Greece

² Department of Information Systems, Statistics, and Management Science, University of Alabama, Tuscaloosa, Alabama, USA

³ Department of Statistics, University of Pretoria, Pretoria, South Africa

⁴ Department of Science, Mathematics and Technology Education, University of Pretoria, Pretoria, South Africa

⁵ School of Mathematical Sciences, Universiti Sains Malaysia, Penang, Malaysia

Abstract

In this paper, we provide an overview of a class of control charts called the synthetic charts. Synthetic charts are a combination of a traditional chart (such as a Shewhart, CUSUM, or EWMA chart) and a conforming run-length (*CRL*) chart. These charts have been considered in order to maintain the simplicity and improve the performance of small and medium-sized shift detection of the traditional Shewhart charts. We distinguish between different types of synthetic-type charts currently available in the literature and highlight how each is designed and implemented in practice. More than 100 publications on univariate and multivariate synthetic-type charts are reviewed here. We end with some concluding remarks and a list of some future research ideas.

Keywords: Conforming run-length (*CRL*), Markov chain, Shewhart chart, Side-sensitive, Steady-state average run-length, Synthetic chart, Zero-state average run-length.

1. INTRODUCTION

Statistical process monitoring (SPM) consists of a collection of statistical techniques and tools which are mainly used for identifying changes in industrial or nonindustrial processes. When only common causes of variation are present, the process is (statistically) in-control (IC). Otherwise, the process is out-of-control (OOC), and one searches for assignable causes of variation. The most popular charts are the Shewhart charts, proposed by Walter A. Shewhart in the 1920s. Despite their simplicity and versatility, one drawback of Shewhart charts is their insensitivity in detecting small and moderate-sized shifts. Thus, various modifications of the Shewhart charts have been considered, focusing on how to increase their sensitivity. Among the charts that focus on improving the traditional Shewhart charts is the synthetic chart. These charts have received and continue to receive a lot of interest from researchers.

Wu and Spedding¹ proposed the first synthetic chart by combining the Shewhart \bar{X} and conforming run-length (*CRL*) subcharts to increase the sensitivity of the Shewhart chart for detecting small and moderate, abrupt shifts in the mean of a normally distributed process, or for brevity, a normal process. The variable *CRL* is defined as the number of units (samples) produced/observed between two consecutive nonconforming units (samples), inclusive of the nonconforming unit (sample) at the end, and a control chart based on the *CRL* statistic is called the *CRL* chart. Bourke² proposed and studied the *CRL* chart in the case of monitoring the percentage

* Correspondence: Subhabrata Chakraborti, Department of Information Systems, Statistics, and Management Science, University of Alabama, Tuscaloosa, AL.
Email: schakrab@cba.ua.edu

of nonconforming items for a high-yield process. This chart triggers an OOC signal for the first time when the CRL is significantly small, say, $CRL \leq H$, where H is a positive integer greater than 0. Thus, H is the control limit of the CRL chart. The rationale behind the CRL chart is the following:

Small CRL values are indicative of less conforming items produced between the two successive nonconforming ones. Consequently, this may be an indication that the process is operating under some assignable causes of variation. For a synthetic chart, an OOC signal is not triggered at the first point that plots on the nonconforming regions; instead, we wait until a second point plots on the nonconforming region and if these two points are not “*far away from each other*,” then the CRL chart signals (ie, the CRL is significantly small) and, consequently, an OOC signal is triggered.

Following the work of Wu and Spedding,¹ Scariano and Calzada³ presented the *generalized synthetic chart (GSC)* methodology by combining any subchart (i.e., instead of the \bar{X} chart, they considered any Shewhart, CUSUM, or EWMA chart) with the CRL subchart. Another key finding on synthetic-type charts was by Davis and Woodall⁴ where the authors noticed that the synthetic chart of Wu and Spedding¹ is just a *2-of-(H+1)* runs-rules chart with a head-start feature. That is, the similarity with runs-rules charts made it easier to formulate and study the theoretical run-length (RL) properties of the synthetic charts.

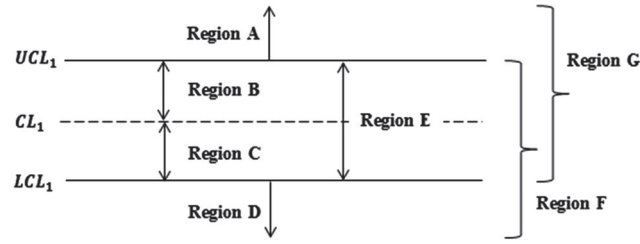
This paper is structured as follows: In Section 2, we give the different types of synthetic charts as well as their operation, zero-, and steady-state RL properties. The available univariate and multivariate synthetic charts are reviewed in Sections 3 to 5. The concluding remarks and topics of future research are given in Section 6.

2. DESIGN OF THE SHEWHART SYNTHETIC CHARTS

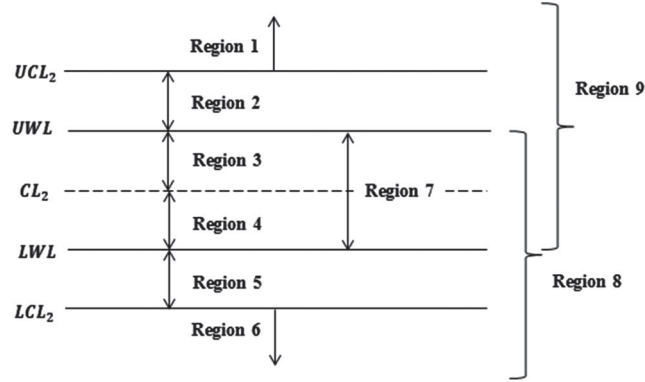
2.1 Types of synthetic charts

There are two main types of synthetic-type control charts, namely, (1) simple synthetic charts and (2) improved synthetic charts. These are based on the charting regions given in Figure 1 A,B, respectively. Furthermore, depending on the type of the first subchart, these two categories are further subdivided into six different types, i.e., for one-sided schemes, there is a lower and an upper; whereas, for the two-sided schemes, there are nonside-sensitive (NSS), standard side-sensitive (SSS), revised side-sensitive (RSS), and modified side-sensitive schemes (MSS). The NSS simple and improved synthetic charts are denoted here as S1 (first proposed by Wu and Spedding¹) and IS1 (first proposed by Wu et al⁵), respectively. Similarly, the SSS, RSS, MSS, simple, and improved synthetic charts are denoted here as S2 (by Davis and Woodall⁴) and IS2, S3 (by Machado and Costa⁶) and IS3 (by Machado and Costa⁷), and S4 (by Shongwe and Graham⁸) and IS4 (by Shongwe and Graham⁹), respectively. Using Figure 1, Table 1 is constructed to distinctly show the different regions that are used to differentiate between these synthetic-type charts. For example, the charting regions of the lower one-sided improved synthetic chart from Figure 1B are regions 5, 6 and 9, where region 9 is a conforming region, region 5 is a nonconforming region, and region 6 is an OOC region—the rest of the schemes in Table 1 (in conjunction with Figure 1) are interpreted in a similar fashion.

Given the regions shown in Figure 1 and Table 1 for each of the distinct schemes, their unified operation is as given in Table 2. So far in the literature, the *GSC* methodology of the EWMA and CUSUM subcharts has only been studied for the S1-type only.



(A) Simple synthetic charts



(B) Improved synthetic charts

FIGURE 1 Control and warning limits for the synthetic-type control charts

2.2 Transition probability matrices and some run-length properties

The transition probability matrix (TPM) is of the form

$$\mathbf{P}_{(M+1) \times (M+1)} = \begin{pmatrix} \mathbf{Q} & \mathbf{r} \\ \mathbf{0}' & 1 \end{pmatrix} \quad (1)$$

where \mathbf{Q} is the $M \times M$ matrix of transient probabilities (called the essential TPM), $\mathbf{0} = (0, 0, \dots, 0)'$ is the $M \times 1$ null vector, and the $M \times 1$ vector \mathbf{r} satisfies $\mathbf{r} = \mathbf{1} - \mathbf{Q}\mathbf{1}$ (ie, row probabilities must sum up to 1) with $\mathbf{1} = (1, 1, \dots, 1)'$. By following a similar procedure of decomposing the elements of the TPMs (see Davis and Woodall⁴), the TPM of the upper or lower one-sided simple and improved synthetic schemes as well as the S1 and IS1 schemes for any value of H is given by

	ϕ	η_2	η_3	η_4	\dots	$\eta_{\tau-1}$	η_{τ}	OOC
ϕ	a	b	0	0	\dots	0	0	c
η_2	0	0	a	0	\dots	0	0	$b+c$
η_3	0	0	0	a	\dots	0	0	$b+c$
\vdots	\vdots	\vdots	\vdots	\vdots	\ddots	\vdots	\vdots	\vdots
$\eta_{\tau-2}$	0	0	0	0	\dots	a	0	$b+c$
$\eta_{\tau-1}$	0	0	0	0	\dots	0	a	$b+c$
η_{τ}	a	0	0	0	\dots	0	0	$b+c$
OOC	0	0	0	0	\dots	0	0	1

TABLE 1 Regions for synthetic-type charts shown in Figure 1

			All Regions	Conforming Regions	Nonconforming Regions	OOO Regions
Simple synthetic charts	One-sided	Lower	D, G	G	D	None
		Upper	A, F	F	A	
	Two-sided	S1 ^a	X, E	E	X	
		S2	A, D, E	E	A, D	
		S3	A, D, E	E	A, D	
S4	A, B, C, D	B, C	A, D			
Improved synthetic charts	One-sided	Lower	5, 6, 9	9	5	6
		Upper	1, 2, 8	8	2	1
	Two-sided	IS1 ^b	Y, 1, 6, 7	7	Y	1, 6
		IS2	1, 2, 5, 6, 7	7	2, 5	1, 6
		IS3	1, 2, 5, 6, 7	7	2, 5	1, 6
		IS4	1, 2, 3, 4, 5, 6	3, 4	2, 5	1, 6

^aX = AUD.

^bY = 2U5.

TABLE 2 Operation of the simple and improved synthetic-type charts

Step	Simple Synthetic Charts	Improved Synthetic Charts
1	Specify the desired value of H .	
2	Compute the applicable limits: $UCL1/CL1/LCL1$	Compute the applicable limits: $UCL2/UWL/CL2/LWL/LCL2$
3	Wait until the next inspection time, take a random sample of size n , and calculate the corresponding plotting statistic, Y_i .	
4	If $Y_i \geq UCL2$ and $Y_i \leq LCL2$, go to step 7.	
5	If the i th sample is conforming, hence return to step 3; otherwise, go to step 6.	
6	Calculate CRL , ie, the number of conforming samples in between the current and next nonconforming sample - inclusive of the nonconforming sample at the end. If $CRL \leq H$, go to step 7; otherwise return to step 3.	
7	Issue an OOC signal and then take necessary corrective action to find and remove the assignable causes. Then return to step 3.	

with each of the probability elements as given in Table 3, $\tau = H + 1$ and assuming that θ_x denotes the probability for a sample point to plot in region x , $x \in \{A, B, \dots, G, X, Y, 1, 2, \dots, 9\}$, i.e., $\theta_x = P(Y_i \in x)$.

Due to space restrictions, the readers are referred to Shongwe and Graham¹⁰ for the TPMs of the S2, S3, and S4, whereas the TPMs of the IS2, IS3, and IS4 are given in Shongwe and Graham.¹¹ Also, M (in Equation (1)) is some specified positive integer that depends on the control limit H of the CRL subchart. For example, for the one-sided simple and improved synthetic charts as well as the S1 and IS1 charts, $M = H + 1$, while for the S2 and IS2 charts, $M = (H + 1)^2$ for the S3 and IS3 charts, $M = 3H + 1$, and for the S4 and IS4 charts, $M = 4H$.

Once the essential TPM Q has been determined, the theoretical properties of the RL distribution can be determined (see Fu and Lou¹²). That is, the probability density function (pdf) $f_{RL}(\ell) = P(RL = \ell)$, the cumulative distribution function (cdf) $F_{RL}(\ell) = P(RL \leq \ell)$, the average run-length ($ARL = E(RL)$), and the standard deviation of the run-length ($SDRL = \sqrt{V(RL)}$) can be calculated via an appropriate Markov chain (MC) technique by using the following formulae:

$$f_{RL}(\ell) = \mathbf{q}'\mathbf{Q}^{\ell-1}\mathbf{r}, \ell = 1, 2, \dots, \quad (2)$$

$$F_{RL}(\ell) = 1 - \mathbf{q}'\mathbf{Q}^{\ell}\mathbf{r}, \ell = 1, 2, \dots, \quad (3)$$

$$ARL = \mathbb{E}(RL) = \mathbf{q}'(\mathbf{I} - \mathbf{Q})^{-1}\mathbf{1}, \quad (4)$$

$$SDRL = \sqrt{\mathbb{V}(RL)} = \sqrt{2\mathbf{q}'(\mathbf{I} - \mathbf{Q})^{-2}\mathbf{Q}\mathbf{1} - ARL^2 + ARL}, \quad (5)$$

where \mathbf{q} is the zero-state initial probability vector. The 100γ ($0 < \gamma < 1$) percentile of the run-length distribution can be determined as the value ℓ_γ such that $F_{RL}(\ell_\gamma - 1) \leq \gamma$ and $F_{RL}(\ell_\gamma) > \gamma$. Clearly, for $\gamma=0.5$, we obtain the median of the RL distribution, i.e., $MRL=\ell_{0.5}$; for a simulation study illustrating the percentile and median RL , see Chong et al.¹³, whereas that illustrating the use of $SDRL$, see Khoo et al.¹⁴ Other popular performance measures in the literature of synthetic charts are (see Calzada and Scariano,¹⁵ Fang et al.,¹⁶ Machado and Costa⁷) the average number of observations to signal ($ANOS$) and the average time to signal (ATS) as well as the extra quadratic loss ($EQL = \int_{\delta_{\min}}^{\delta_{\max}} \delta^2 ARL(\delta)h(\delta)d\delta$) and the expected ARL ($EARL = \int_{\delta_{\min}}^{\delta_{\max}} ARL(\delta)h(\delta)d\delta$) where $ARL(\delta)$ is the average run-length as a function of the shift δ in the parameter under surveillance, and δ_{\min} and δ_{\max} are, respectively, the lower and upper bounds of δ . Moreover, the shifts within the interval $[\delta_{\min}, \delta_{\max}]$ occur according to a probability distribution with pdf equal to $h(\delta)$.

TABLE 3 The probability elements for the TPM of the one-sided and two-sided NSS simple and improved synthetic-type charts

	Type		a	b	c
Simple synthetic chart	One-sided	Lower	θ_G	θ_D	0
		Upper	θ_F	θ_A	0
	Two-sided	S1	θ_E	θ_X	0
Improved synthetic chart	One-sided	Lower	θ_9	θ_5	θ_6
		Upper	θ_8	θ_2	θ_1
	Two-sided	IS1	θ_7	θ_Y	$\theta_1+\theta_6$

2.3 Zero-state and steady-state modes

Davis and Woodall⁴ showed that the RL distribution of the synthetic chart can be very different under the *zero-state* and *steady-state* modes. In the zero-state mode, it is assumed that the shift in the process parameter(s) has occurred exactly at the time the monitoring starts so that there is a nonconforming sample at time zero. Thus, the occurrence of another nonconforming sample within the next H samples will give an OOC signal. According to Davis and Woodall,⁴ this engenders a head-start feature, and this is why the S1 chart appears to be more powerful than several popular competing charts. On the other hand, in the steady-state mode, one assumes that the process starts and stays IC for a “long” time period, so as the effect of the head-start feature disappears; a process shift occurs at some “random time.” Without the head-start feature, as Davis and Woodall⁴ also showed, the RL performance of the synthetic chart declines. This fact has also been cited as a reason against the use of synthetic charts.

To obtain the steady-state performance of the synthetic chart, the vector \mathbf{q} has to be replaced by the vector \mathbf{s} (in Equations (2) to (5)) that consists of the percentage of time, over *many samples* under the IC state that the Markov chain will be in each transient state. In order to obtain \mathbf{s} , two approaches are considered (see Knoth¹⁷). These are as follows: (1) The vector \mathbf{s} consists of the

percentage of time that the Markov chain will be in each transient state, given that no false alarm was raised before the actual process shift. This is known as the *conditional* setup and gives the *conditional steady-state* performance of the chart. (2) It is assumed that instead of conditioning on false alarm, the actual process shift may happen after a sequence of false alarms; after each false alarm, the chart is restarted. This is known as the *cyclical* setup and gives the *cyclical steady-state* performance. For a comparison of these different types of steady-state methods, readers are referred to Davis and Woodall,⁴ Knoth,¹⁷ and Machado and Costa.^{6,7}

2.3 Zero-state and steady-state run-length closed-form expressions

Scariano and Calzada³ and Calzada and Scariano¹⁵ showed that the zero-state *ARL* and *SDRL* of the S1 chart are equal to

$$ARL_{ZS} = \frac{1}{\theta_X(\delta)(1-(1-\theta_X(\delta))^H)}, \quad (6)$$

$$SDRL_{ZS} = \sqrt{\frac{2-\theta_X(\delta)}{(1-(1-\theta_X(\delta))^H)(\theta_X(\delta))^2} + \frac{\frac{1}{(\theta_X(\delta))^2} - 2 \sum_{l=1}^H l(1-\theta_X(\delta))^{l-1}}{(1-(1-\theta_X(\delta))^H)^2}}, \quad (7)$$

respectively, where $\theta_X(\delta)$ denotes the probability θ_X (see Table 3) as a function of the shift parameter δ . The ARL_{ZS} and $SDRL_{ZS}$ are also functions of δ . In order to keep the notation simple, we use ARL_{ZS} and $SDRL_{ZS}$ instead of $ARL_{ZS}(\delta)$ and $SDRL_{ZS}(\delta)$, respectively. The steady-state *ARL* and *SDRL* are denoted as ARL_{SS} and $SDRL_{SS}$, respectively. The advantage of using Equations (6) and (7) is that the zero-state *ARL* and *SDRL* can be calculated directly without matrix inversion. On the other hand, with the Markov chain approach, the entire *RL* distribution is available, which may be more attractive and comprehensive to study chart performance. For an analytical expression of the (cyclical) steady-state *ARL* of the S1 chart, Wu et al⁵ developed the formula

$$ARL_{SS} = \frac{1}{\theta_X(\delta)} - 0.5 + (1 - \psi)ARL_{ZS}, \quad (8)$$

where

$$\psi = \frac{\theta_X(\delta)(1-\theta_X(0))(1-(1-\theta_X(0))^H) - \theta_X(0)(1-\theta_X(\delta))(1-(1-\theta_X(\delta))^H)}{\theta_X(\delta) - \theta_X(0)}.$$

$\theta_X(0)$ is the θ_X calculated at the IC state. Also, the steady-state *ARL* of the S1 chart under the conditional setup is given by (see Knoth¹⁷)

$$ARL_{SS} = \left(\frac{\varrho_0}{\theta_X(0)} + \frac{1-(1-\xi_0)^H}{\xi_0} \right) \frac{\xi_0}{\theta_X(\delta)} + \left(\frac{\varrho_0}{\theta_X(0)} + (1 - \theta_X(\delta))^H \frac{1-\left(\frac{1-\xi_0}{1-\theta_X(\delta)}\right)^H}{1-\frac{1-\xi_0}{1-\theta_X(\delta)}} \right) \xi_0 ARL_{ZS}, \quad (9)$$

where ϱ_0 is the largest eigenvalue of the essential TPM \mathbf{Q} when the process is IC and $\xi_0 = 1 - (1 - \theta_X(0))/\varrho_0$.

More general expressions for the zero-state *ARL* and *SDRL* of the S1 chart were provided by Scariano and Calzada³ in the case of the *GSC*. These formulae are

$$ARL_{GSC} = \frac{1}{P(RL \leq H)} \mathbb{E}(RL), \quad (10)$$

$$SDRL_{GSC} = \left(\frac{1}{P(RL \leq H)} \mathbb{E}(RL^2) + \frac{1}{(P(RL \leq H))^2} \mathbb{E}(RL) \{ \mathbb{E}(RL) - 2 \sum_{\ell=1}^H \ell \cdot P(RL = \ell) \} \right)^{1/2}, \quad (11)$$

where RL is the run-length random variable of the first subchart. The approach of Scariano and Calzada³ has led researchers to combine one of the most popular schemes (Shewhart, CUSUM, or EWMA) with the CRL chart. For the case of the Shewhart \bar{X} chart as the first subchart, we have

$$\mathbb{E}(RL) = \frac{1}{\theta_X(\delta)}, \quad \mathbb{E}(RL^2) = \frac{2 - \theta_X(\delta)}{\theta_X^2(\delta)}, \quad P(RL = \ell) = (1 - \theta_X(\delta))^{\ell-1} \theta_X(\delta)$$

and from direct substitution into Equations (10) and (11), we obtain Equations (6) and (7).

Note that the expressions in Equations (6) to (11) can easily be shown (in a similar fashion as done in Section 2.2 for the given unified TPM) that they correspond to the lower and upper one-sided simple and improved synthetic charts as well as the S1 and IS1 schemes only. For the ARL_{SS} of the S3 and IS3 charts, the reader is referred to Machado and Costa,^{6,7} respectively.

2.5 Statistical design of synthetic charts

Wu and Spedding¹ gave an algorithm to implement the optimal design (i.e., a search for the parameters (k, H) such that a specific IC RL value is attained) for the S1 chart. Usually, $k > 0$ is a charting constant that is related to the distance of the UCL_1/LCL_1 from CL_1 , in terms of standard deviation. Similar approaches for the design of the S2, S3, and S4 charts are also available (see, for example, Machado and Costa⁶). Next, Wu et al⁵ similarly gave an implementation algorithm (ie, a search for the parameters (k_1, k_2, H) such that a specific IC RL value is attained) for the IS1 chart, with $k_1 > k_2 > 0$, the charting constants that are related to the distance of the $UCL_2/UWL/LWL/LCL_2$ from CL_2 , in terms of standard deviation. Similar approaches for the design of the IS2, IS3, and IS4 charts are also available (see, for example, Machado and Costa⁷). A different algorithm was proposed in Aparisi and de Luna,¹⁸ so that the synthetic chart may only detect the shifts that are considered as important by the practitioners. However, if the practitioner has no historical data to estimate the important shifts, say δ^* on the process parameter(s), the Taguchi loss function approach (Aparisi and García-Díaz¹⁹) can be used to determine the important regions.

3 LITERATURE REVIEW

A brief review of univariate S1 charts used for monitoring the mean and those used for monitoring the variance was given in Khoo.²⁰ Specifically, Khoo²⁰ discussed the S1 chart for monitoring the mean for skewed distributions (Khoo et al,²¹ Castagliola and Khoo²²), its robustness to non-normality (Calzada and Scariano²³), and the S1 chart combined with double sampling (DS) (Khoo et al²⁴). Thus, papers already reviewed by Khoo²⁰ will not be discussed in detail here but will only be mentioned briefly. In the literature, there are several synthetic charts, which are suitable for monitoring various processes, under different settings. These charts are summarized in Table 4, and its structure is used for reviewing these charts in Sections 3 to 5.

3.1 Synthetic charts for monitoring the mean of a normal process

Khoo et al²⁵ studied the statistical design of the S1 chart based on the *MRL* under the zero- and steady-state modes. Note that in all the above articles, it is assumed that the underlying process parameters are known (this is known as case K); however, when the process parameters are unknown, they must be estimated in phase I before the start of monitoring in phase II (this is known as case U). Zhang et al²⁶ were the first who studied the effect of parameter estimation on synthetic charts for the normal mean in case U where they investigated the effect of parameter estimation on the S1 chart. Their analysis revealed that the unconditional *RL* properties in case U can be significantly different from those in case K (especially when the number of phase I samples is small), making it inappropriate to use the optimal charting constants k and H that corresponds to case K in case U. Recently, Hu et al²⁷ studied the S1 chart in case U by modifying the k value using the bootstrap method in order to have a conditional guaranteed IC performance.

Extending on the S1 DS work by Khoo et al,²⁴ You et al²⁸ studied the corresponding case U. Note that the latter two articles used the *ARL* as the design criterion. You^{29,30} noted that designing control charts using the *ARL* requires practitioners to specify the target shift size in advance, and consequently, if this is unknown (or the shift size is random), then the *EARL* is more appropriate. Consequently, You,^{29,30} respectively, designed the S1 DS chart in case K and case U using the *EARL*. Finally, Costa and Machado³¹ and Malela-Majika and Rapoo,³² respectively, studied the S3 and S4 DS charts in case K.

When errors in estimating the process standard deviation exist, either due to inadequate/unreliable IC data or due to changes in the process standard deviation (i.e., the \bar{X} chart suffers from a wide variation in the desired IC *ARL* values), Calzada and Scariano¹⁵ proposed two S1-type charts based on the Student's t distribution: one with the t and the other with the EWMA- t subchart in order to monitor the process mean under the zero-state mode, as these do not require estimation of the standard deviation from reference samples. The S1 t chart in case U was studied by Teoh et al,³³ under both zero- and steady-state modes. They also provided the appropriate (k , H) values for its optimal design according to the zero- and steady-state *ARL* as well as the *EARL*.

There are some adaptive synthetic charts that exist in the literature. Lim³⁴ investigated the zero- and steady-state S1 scheme where the *CRL* is calculated using larger sample sizes and shorter sampling intervals. Song and Park³⁵ and Lee et al³⁶ studied the steady-state and zero-state of the variable sampling interval (VSI) IS1 charts, respectively. Lee and Lim³⁷ and Yu et al³⁸ investigated the variable sample size and interval (VSSI) using the S1 and IS1 charts, respectively. Costa and Machado³⁹ studied the steady-state IS1 and IS3 charts with a variable sample size (VSS). Other works on synthetic charts for monitoring the mean of a normal process consist of the study of the effect of measurement errors on the performance of the S1 chart by Hu et al⁴⁰ and the study of the auxiliary-based information on the S1-type Shewhart chart by Haq and Khoo⁴¹ and EWMA as well as CUSUM charts by Haq,⁴² respectively. The only work on univariate synthetic charts for monitoring non-IID data is from Hu and Sun⁴³ who studied the performance of the S1 chart for an autoregressive process of order 1.

TABLE 4 Classification of synthetic charts according to their use

Synthetic Chart	Quality Characteristic/Process Parameter/Design Type	Section
For variables (parametric setup)	Mean	3.1
	Variance	3.2
	Mean and variance (joint monitoring)	3.3
	Mean time between events	3.4
	Economic and economic-statistical designs	3.5
For attributes	Fraction/number of nonconforming	4
	Average/actual number of nonconformities	
Multivariate processes	Mean vector	5
	Covariance matrix	
	Vector of the number of nonconforming items	

Finally, using ranked sampling methods such as the ranked set sampling (RSS), median RSS, and order RSS (see, for example, Mutlak and Al-Sabah⁴⁴), Haq et al^{45,46} studied the usual S1 as well as the S1 EWMA and S1 CUSUM charts for process mean and found out that they outperform their counterparts based on simple random sampling (SRS).

3.2 Synthetic charts for monitoring the variation

Chen and Huang⁴⁷ and Huang and Chen⁴⁸ studied S1 charts based on the sample range R and the sample standard deviation S , respectively. They only studied the zero-state performance of these S1 charts. They also integrated the VSI feature on both subcharts. Rajmanya and Ghute^{49,50} proposed the S1 D -chart based on Downton's estimator

$$D = \frac{2\sqrt{\pi}}{n(n-1)} \sum_{j=1}^n \left(j - \frac{1}{2}(n+1) \right) X_{(j)},$$

where $X_{(j)}$ denotes the j th order statistic in the sample X_1, X_2, \dots, X_n , for $j = 1, 2, \dots, n$. The numerical comparisons of Rajmanya and Ghute^{49,50} revealed that the S1 D -chart produced significant improvement, in terms of ARL_{ZS} , as compared with the R , S , and D charts, as well as to the S1 charts of Chen and Huang⁴⁷ and Huang and Chen⁴⁸ for normally distributed data. The effect of non-normality on the Downton's estimator was also examined. Recently, Guo et al⁵¹ studied a S1 chart based on the S^2 statistic, in both case K and case U. Finally, a S1 DS S chart was recently studied by Lee and Khoo.⁵² No reported works for S2 to S4 and IS1 to IS4 charts in the case of monitoring the variability of a normal process were found in the literature. The usual S1 as well as the S1 EWMA chart for process variation under RSS and MRSS policies were studied by Haq et al^{45,53} and found out that they outperform their counterparts based on SRS.

Before closing this section, it is worth noting that in cases where the process mean and standard deviation may not be constant in the IC state but the latter is proportional to the former, it is more reasonable to monitor the coefficient of variation (CV), ie, $\omega = \sigma/\mu$ of the process. Calzada and Scariano⁵⁴ proposed an upper one-sided S1 chart to monitor increases in ω under the zero-state mode in case K. The charting statistic of the Shewhart-type CV subchart is $W_i = S_i/\bar{X}_i$, $i = 1, 2, \dots$. More recently, Tran et al⁵⁵ studied the latter S1 scheme in the presence of measurement errors.

3.3 Synthetic charts for the joint monitoring of mean and variance

It may be necessary to monitor both the mean (shifting from μ_0 to $\mu_1 = \mu_0 \pm \delta\sigma_0$, where $\delta \neq 0$) and the standard deviation (shifting from σ_0 to $\sigma_1 = \tau\sigma_0$, where $0 < \tau \neq 1$). The usual case is to monitor

a process in order to detect a shift in the process mean, and an increase (i.e., $\tau > 1$) in the variance, or both. For $\tau < 1$, a decrease in the process standard deviation has occurred. In the literature, there are four S1 charts for monitoring the mean and variance simultaneously using one charting statistic instead of two separate charting statistics. Costa and Rahim⁵⁶ proposed and studied a S1 chart based on the noncentral chi-square (NCS) statistic, i.e.,

$$T_i = \sum_{j=1}^n (X_{ij} - \mu_0 + \xi_i \sigma_0)^2, \quad i = 1, 2, \dots,$$

where $\xi_i = d$ if $X_{ij} > \mu_0$; otherwise, $\xi_i = -d$, where $d > 0$ is a positive constant. Chen and Huang⁵⁷ proposed a S1 chart based on the $M = \max \{|U|, V\}$ statistic, where

$$U = \sqrt{n}(\bar{X} - \mu_0)/\sigma_0, \quad V = \Phi^{-1}\{F_{n-1}((n-1)S^2/\sigma_0^2)\}$$

and $\Phi(\cdot)$, $F_{n-1}(\cdot)$ are the cdf of the standard normal distribution and the chi-square distribution with $n-1$ degrees of freedom, respectively. Costa et al⁵⁸ studied a S1 chart based on the NCS statistic with two-stage testing, and more recently, Lee and Khoo⁵⁹ studied the mean square error (MSE) S1 chart based on the statistic

$$MSE_i = S_i^2 + \frac{n(\bar{X}_i - T_0)^2}{n-1}$$

where T_0 is the target value of the process. Finally, Machado and Costa⁷ studied the steady-state performance of the IS3 chart that utilizes the joint $X\&R$ chart as the first subchart. Except for the latter, all other charts are of the S1 type, and their performances were evaluated under the zero-state mode. The numerical analysis revealed that each synthetic chart discussed here outperforms its nonsynthetic counterpart.

3.4 Synthetic charts for monitoring the mean time between events

In some high-quality processes, it is often recommended that one monitors the time between events (failures) and not the number of events (e.g., nonconforming items), since they rarely occur. Scariano and Calzada⁶⁰ were the first to propose a lower one-sided simple synthetic chart for monitoring the mean time between events (failures) (TBE) assuming an exponential distribution. Fang et al¹⁶ proposed a lower one-sided chart which consists of the t_r chart as the first subchart (for monitoring the mean TBE in the case of a homogenous Poisson process). They evaluated its performance in terms of the *ANOS*, since in TBE charts, a single point does not consist of a single observation but requires r consecutive, usually exponentially distributed observations. Fang et al¹⁶ showed that, in terms of the zero-state *ANOS*, the lower one-sided chart based on the Erlang distribution with $r = 4$ outperforms the exponential-EWMA chart for all the considered shifts in the mean TBE. Furthermore, in terms of the steady-state *ANOS*, the lower one-sided chart with $r = 5$ chart as the first subchart is more efficient than the exponential-EWMA chart in detecting small to moderate shifts. The S1 exponential charts in case U have been studied by Cheng et al⁶¹ and Sun et al,⁶² respectively; the former provides a phase II *ARL*-unbiased design while the latter gives an exact method for guaranteed IC performance.

3.5 Economic and economic-statistical designs for synthetic charts

Yeong et al⁶³ proposed the first economic model for the S1 chart in which they formulated an algorithm to find the optimal values of the chart's design parameters, which minimize the net sum of all costs involved, so that the chart can be operated at an economically optimal level by using the approximation of the cost function in Chung.⁶⁴ Recently, Yeong et al⁶⁵ further showed the

economic efficiency of the S1 \bar{X} chart as compared with that of the ordinary \bar{X} chart. A sensitivity analysis was done by Yeong et al⁶³ and Yeong and Khoo.⁶⁶ Both papers stressed that sometimes it is not feasible to operate the chart at the economically optimal point. However, they provided conditions where the saving is larger when the S1 \bar{X} chart is adopted instead of the ordinary \bar{X} chart. The economic and economic-statistical designs of the S1 chart in case K and case U were studied by Yeong et al⁶⁷ and Yeong et al,⁶⁸ respectively. The economic and economic-statistical design of the S1 DS \bar{X} chart of Khoo et al²⁴ was studied by Lee and Khoo.⁶⁹ A corresponding economic design of a slightly modified S1 DS \bar{X} chart was done by Aghaulor and Ezekwem.⁷⁰ In the case of monitoring process variation, the economic design of the upper one-sided chart of Guo et al⁵¹ in the presence of measurement errors was studied by Hu et al.⁷¹ Lee and Khoo⁷² provided the economic-statistical design of the S1 Max chart of Chen and Huang.⁵⁷ Finally, Wan et al⁷³ studied the integrated economic design of the adaptive IS1 chart of Yu et al³⁸ and the maintenance management system.

4 SYNTHETIC CHARTS FOR ATTRIBUTE DATA

Wu et al⁷⁴ presented the design, operation, and *ATS* performance for the S1 chart with a *np* subchart and showed that it has an improved zero-state performance than the traditional *np* chart. Bourke⁷⁵ showed that, in zero state, the apparent superior performance reported in Wu et al⁷⁴ is due to a limited choice of circumstances for making comparisons. Moreover, in the steady-state mode, the advantage of the S1 chart over the *np* chart is at most 3%, which is not significant enough to adopt the more complicated S1 chart. Following Wu et al,⁵ Haridy et al⁷⁶ proposed a IS1 chart with the *np* chart as the first subchart. The authors showed that, overall, the IS1 chart is more effective than the *np* chart and the S1 *np* chart. The effect of parameter estimation on S1 attributes charts was studied by Castagliola et al⁷⁷ by evaluating the *RL* properties of the S1 *p*, *np*, *c*, and *u* charts using the MC approach in case K as well as in case U. Recently, Lee and Khoo⁷⁸ studied the statistical design of the S1 *np* chart based on the *MRL*. Chong et al⁷⁹ proposed and studied the S1 DS chart with the *np* chart as the first subchart, which can be viewed as the attribute analogue of the S1 DS \bar{X} chart of Khoo et al.²⁴ Finally, Adnaik and Gadre⁸⁰ designed the zero-state and steady-state Markov chain procedure for S1 *np* chart in the case of autocorrelated binary observations according to a first-order Markov dependence.

5 MULTIVARIATE SYNTHETIC CHARTS

When more than one correlated characteristics are to be monitored, multivariate charts must be used. The term multivariate synthetic chart refers to a scheme that consists of a multivariate chart as the first subchart and the *CRL* chart as the second subchart. Under the assumption of normality, Ghute and Shirke⁸¹ as well as Aparisi and de Luna⁸² integrated the Hotelling's T^2 chart and the *CRL* chart to form the synthetic T^2 or S1 T^2 chart. The authors evaluated its performance under the zero-state mode and showed that the S1 T^2 chart increases the sensitivity of the Hotelling's T^2 chart in detecting shifts in the mean vector. Khoo et al⁸³ presented a multivariate S1 chart for monitoring the process mean vector of skewed populations, using the weighted standard deviation method. Khoo et al⁸⁴ studied the statistical design of the S1 T^2 chart based on the *MRL* criterion. The authors showed numerically that, under the zero-state mode, the S1 T^2 chart outperforms the multivariate EWMA chart, for moderate and large shifts. However, under the steady-state mode, the multivariate EWMA is more superior, and their performance is only comparable for very large shifts. Khoo et al⁸⁵ proposed the S1 DS T^2 chart and noted that it outperforms the multivariate EWMA chart for moderate and large shifts, but the latter is superior for small shifts. Moreover, the S1 DS T^2 chart generally outperforms the basic T^2 , S1 T^2 , and DS T^2 charts. Yeong et al⁸⁶ studied the economically optimal design of the S1 T^2 chart. There are no other synthetic-type T^2 charts based on the S2 to S4 and IS1 to IS4 designs that have been reported in the literature so far.

Simões et al⁸⁷ studied the performance of the S1 T^2 chart in the case of a bivariate autocorrelated process. Moreover, the authors considered the S3 scheme with the joint X (one for each variable) subchart. Their numerical comparisons showed that the autocorrelation has a negative effect on the side-sensitive schemes and they are inferior to the usual S1 T^2 chart, especially for variables with a high correlation coefficient. Costa and Machado⁸⁸ considered a correlated bivariate process using a two-stage sampling procedure with a S1 T^2 chart. More recently, Dargopatil and Ghute⁸⁹ proposed a multivariate analogue of Hu and Sun⁴³ using skipping and mixed sampling strategies to reduce the negative effect of autocorrelation. It seems that these are the only works on synthetic charts for monitoring a multivariate process with non-IID observations.

Recently, Celano and Castagliola⁹⁰ proposed a S1 chart, the Syn-RZ chart, where the first subchart is a Shewhart-type one based on the ratio $Z = X_1/X_2$ of a bivariate normal process with process mean vector $\boldsymbol{\mu}_X = (\mu_{X_1}, \mu_{X_2})$ with correlation coefficient ρ between X_1 and X_2 . This chart is suitable for detecting shifts in the ratio μ_{X_1}/μ_{X_2} as well as on ρ . Other multivariate synthetic charts reported in the literature include the S1 chart based on the VMAX statistic by Machado et al,⁹¹ which can be used for monitoring the covariance matrix $\boldsymbol{\Sigma}$ of a bivariate normal process. The proposed charting statistic utilizes the sample variances of two correlated random variables, i.e.

$$\text{VMAX} = \max\{S_x^2, S_y^2\},$$

where $S_x^2 = \sum_{i=1}^n x_i^2/n$, $S_y^2 = \sum_{i=1}^n y_i^2/n$ and (x_i, y_i) , $i = 1, 2, \dots, n$, is a sample of size n from a bivariate normal process with covariance matrix $\boldsymbol{\Sigma}$. Furthermore, Ghute and Shirke⁹² proposed and studied the S1 $|\mathbf{S}|$ chart for process dispersion by integrating the generalized sample variance $|\mathbf{S}|$ chart and the CRL chart. A VSI version of this scheme was studied by Lee and Khoo.⁹³ Recently, Lee and Khoo⁹⁴ proposed a zero- and steady-state IS1 $|\mathbf{S}|$ chart, and Lee and Khoo⁹⁵ designed the S1 $|\mathbf{S}|$ chart based on the MRL criterion. Ghute and Shirke⁹⁶ proposed the S1 T^2 and $|\mathbf{S}|$ subchart (to jointly monitor the multivariate mean and variability) and the CRL chart in zero state and showed that it has a superior OOC performance than its nonsynthetic counterparts.

The S1 E-chart (Liu et al⁹⁷) combines the chart based on conditional entropy of Guerrero-Cusumano⁹⁸ with the CRL chart. Using the concept of the GSC of Scariano and Calzada,³ Lee⁹⁹ developed a S1 multivariate EWMA chart by considering the multivariate EWMA chart as a subchart while a S1 multivariate CUSUM chart was studied by Lee et al.¹⁰⁰ Extensive numerical comparisons showed that under the steady-state mode, these S1 multivariate charts outperform their nonsynthetic counterparts in detecting shifts in the process mean vector. Finally, for multiattribute processes, Haridy et al¹⁰¹ proposed and studied a multiattribute synthetic- np chart. Two different types of synthetic charts, a S1 and an IS1, were established by combining the multiattribute np chart with the CRL chart, and their performance was evaluated under the steady-state mode.

6 CONCLUDING REMARKS AND FUTURE RESEARCH

In this paper, the available literature on different types of synthetic charts is reviewed. Both univariate and multivariate synthetic charts have been covered. Synthetic charts can be useful for the quality practitioner in a variety of applications. The signaling rule of the synthetic-type chart is useful for practitioners who may want to wait for a second point plotting on the nonconforming region, before declaring a process OOC. The reported results in the literature reveal that the Shewhart synthetic charts that signal when two points plot beyond the control limits but on opposite sides of the center line (i.e., not the side-sensitive rule) are not as efficient as those that are side-sensitive. On the contrary, one of the reasons why no synthetic EWMA and CUSUM charts

based on the S2 to S4 and IS2 to IS4 designs exists is because Khoo et al¹⁰² found that the side-sensitive EWMA runs-rules schemes do not offer any improvement over their non-side-sensitive counterparts.

Finally, in addition to the suggestions for future research given in Khoo,²⁰ we provide a summary of some topics that have not yet been addressed or have only been partially addressed.

1. The zero-state performance metrics for the synthetic chart can be misleading, due to its inherent head-start feature. We suggest that researchers should evaluate the performance of synthetic charts under the steady-state mode, especially in the case of numerical comparisons between competitive schemes. In fact, recent works (especially from 2010 onwards) evaluated the performance of synthetic charts under both modes.

2. Although there are some nonparametric synthetic schemes available in the literature (see, for example, Chakraborti and Graham¹⁰³), more work needs to be done.

3. Most of the research on synthetic charts is focused on the basic S1 design, which has been extensively studied for almost every different process, either in case K or case U. However, not much attention has been paid to the S2 to S4 and IS1 to IS4 designs (neither in case K nor in case U, except for the normal mean in case K). It has been proven numerically that for normal processes, the SS schemes outperform the NSS ones. However, this needs to be investigated for non-normal processes, as well.

4. Recent works focus much more on the extensions of the traditional S1 to S4 and IS1 to IS4 charts, with appropriate generalizations of the *CRL* subchart. Instead of the *CRL* chart, the group conforming run-length (*GCRL*) is used (Gadre and Rattihalli¹⁰⁴), and a new class of synthetic charts can be defined, often termed as group runs control chart. For recent work on these charts, see Saha et al¹⁰⁵ and the references therein. These schemes are superior to the reviewed synthetic charts, but this comes with an increased complexity, especially in their statistical design, since at least three or four design parameters must be determined. Even the IS1 to IS4 charts have three design parameters. Traditionally, the most sensitive schemes in the detection of small and moderate shifts are the CUSUM and the EWMA charts. Both require the determination of two design parameters in each. Therefore, in numerical comparisons, the CUSUM and EWMA charts must be included and the improvement attained by the proposed synthetic-type schemes must justify their complexity.

5. Even though recently there was an advisement against the use of synthetic-type charts (see Knoth¹⁷), we believe more research is needed to improve understanding. This is because Knoth¹⁷ only considered the S1 chart in his comparison. From the present overview, there are at least seven more synthetic-type charts (simple and improved), and more synthetic charts can be defined under the *GSC* methodology. Thus, an extended comparison is needed on the zero- and the steady-state performance of all these different synthetic charts with the traditional CUSUM and EWMA charts (see also bulleted item 4 above).

6. If the size of a specific shift a user wants to detect is unknown, then a synthetic chart designed on some specific magnitude shift would perform poorly when the actual magnitude differs significantly from the assumed one. Consequently, in the literature, there has been overall performance metrics that are recommended, i.e., *EQL*, *EARL*, etc. (see Machado and Costa^{6,7} and You^{29,30}). While these articles consider overall performance metrics, most articles considered in this paper only use specific shift performance metrics. Thus, there is still room to assess the performance of the existing and future synthetic monitoring schemes using overall performance metrics. Finally, from a practical standpoint, the control charting procedures must be made more accessible to the practitioner, and to this end, the ease of implementation is vital. Computer

programs, add-ons to popular software packages such as R, or any other commercial or noncommercial software would greatly help in this effort.

In conclusion, even though the synthetic charts have drawn some criticisms in the literature, they continue to attract the attention of researchers and experts in SPM. Thus, modifications, enhancements, and adjustments of synthetic charts have become available in the literature in a steady stream over the last few years. We expect that our overview will shed more light on what has happened until now and would facilitate further research in this area.

ACKNOWLEDGMENTS

The authors would like to thank the two anonymous reviewers for their comments which have helped improve many facets of the presentation and the content of the paper. The work of the third author was financially supported by the South African Researchers Chair Initiative (SARCHI) Chair at the University of Pretoria. Comments by many colleagues are gratefully acknowledged.

REFERENCES

1. Wu Z, Spedding TA. A synthetic control chart for detecting small shifts in the process mean. *J Qual Technol.* 2000;32(1):32-38.
2. Bourke PD. Detecting a shift in fraction nonconforming using run-length control charts with 100% inspection. *J Qual Technol.* 1991;23(3):225-238.
3. Scariano SM, Calzada ME. The generalized synthetic chart. *Seq Anal Des Methods Appl.* 2009;28(1):54-68.
4. Davis RB, Woodall WH. Evaluating and improving the synthetic control chart. *J Qual Technol.* 2002;34(2):200-208.
5. Wu Z, Ou Y, Castagliola P, Khoo MBC. A combined synthetic & \bar{X} chart for monitoring the process mean. *Int J Prod Res.* 2010;48(24):7423-7436.
6. Machado MAG, Costa AFB. Some comments regarding the synthetic chart. *Commun Stat Theory Methods.* 2014;43(14):2897-2906.
7. Machado MAG, Costa AFB. A side-sensitive synthetic chart combined with an \bar{X} chart. *Int J Prod Res.* 2014;52(11):3404-3416.
8. Shongwe SC, Graham MA. A modified side-sensitive synthetic chart to monitor the process mean. *Qual Technol Quan Manag.* 2018;15(3):328-353.
9. Shongwe SC, Graham MA. On the performance of Shewhart-type synthetic and runs-rules charts combined with an \bar{X} chart. *Qual Reliab Eng Int.* 2016;32(4):1357-1379.
10. Shongwe SC, Graham MA. Some theoretical comments regarding the run-length properties of the synthetic and runs-rules monitoring schemes – part 1: zero-state. *Qual Technol Quan Manag.* 2018;16(2):170-189. <https://doi.org/10.1080/16843703.2017.1389141>
11. Shongwe SC, Graham MA. Synthetic and runs-rules charts combined with an \bar{X} chart: Theoretical discussion. *Qual Reliab Eng Int.* 2017;33(1):7-35.

12. Fu JC, Lou WYW. *Distribution theory of runs and patterns and its applications: a finite Markov chain imbedding approach*. Singapore: World Scientific Publishing; 2003.
13. Chong ZL, Khoo MBC, You HW. A study on the run length distribution of synthetic X chart. *Int J Eng Technol*. 2016;8(5):371-374.
14. Khoo MBC, Teh SY, Chew XY, Teoh WL. Standard deviation of the run length (SDRL) and average run length (ARL) performances of EWMA and synthetic charts. *Int J Eng Technol*. 2015;7(6):513-516.
15. Calzada ME, Scariano SM. The synthetic t and synthetic EWMA t charts. *Qual Technol Quan Manag*. 2013;10(1):37-56.
16. Fang YY, Khoo MBC, Lee MH. Synthetic-type control charts for time-between-events monitoring. *PLoS ONE*. 2013;8(6):1-13.
17. Knoth S. The case against the use of synthetic control charts. *J Qual Technol*. 2016;48(2):178-195.
18. Aparisi F, de Luna MA. Synthetic \bar{X} control charts optimized for in-control and out-of-control regions. *Comput Oper Res*. 2009;36(12):3204-3214.
19. Aparisi F, García-Díaz JC. Design and optimization of EWMA control charts for in-control, indifference, and out-of-control regions. *Comput Oper Res*. 2007;34(7):2096-2108.
20. Khoo MBC. Recent developments on synthetic control charts. *Proceedings of the IEEE Symposium on Business, Engineering and Industrial Applications*, 2013;460-465.
21. Khoo MBC, Wu Z, Atta AMA. A synthetic control chart for monitoring the process mean of skewed populations based on the weighted variance method. *Int J Reliab Qual Saf Eng*. 2008;15(3):217-245.
22. Castagliola P, Khoo MBC. A synthetic scaled weighted variance control chart for monitoring the process mean of skewed populations. *Commun Stat Simul Comput*. 2009;38(8):1659-1674.
23. Calzada ME, Scariano SM. The robustness of the synthetic control chart to non-normality. *Commun Stat Simul Comput*. 2001;30(2):311-326.
24. Khoo MBC, Lee HC, Wu Z, Chen C-H, Castagliola P. A synthetic double sampling control chart for the process mean. *IIE Trans*. 2010;43(1):23-38.
25. Khoo MBC, Wong VH, Wu Z, Castagliola P. Optimal design of the synthetic chart for the process mean based on the median run length. *IIE Trans*. 2012;44(9):765-779.
26. Zhang Y, Castagliola P, Wu Z, Khoo MBC. The synthetic X chart with estimated parameters. *IIE Trans*. 2011;43(9):676-687.
27. Hu XL, Castagliola P, Ma YZ, Huang WD. Guaranteed in-control performance of the Synthetic X chart with estimated parameters. *Qual Reliab Eng Int*. 2018;34(5):759-771.
28. You HW, Khoo MBC, Lee MH, Castagliola P. Synthetic double sampling X charts with estimated

parameters. *Qual Technol Quan Manag.* 2015;12(4):579-604.

29. You HW. Run length distribution of synthetic double sampling chart. *Int J Appl Eng.* 2017;12(24):14268-14272.
30. You HW. Performance of the synthetic double sampling chart with estimated parameters based on expected average run length. *J Prob Stat.* 2018;2018:1-6.
<https://doi.org/10.1155/2018/7583610>
31. Costa AFB, Machado MAG. The steady-state behavior of the synthetic and side-sensitive double sampling X charts. *Qual Reliab Eng Int.* 2015;31(2):297-303.
32. Malela-Majika J-C, Rapoo EM. Side-sensitive synthetic double sampling X control charts. *Eur J Ind Eng.* 2018;13(1):117-148.
33. Teoh WL, Chuah SK, Khoo MBC, Castagliola P, Yeong WC. Optimal designs of the synthetic t chart with estimated process mean. *Comput Ind Eng.* 2017;112:409-425.
34. Lim T. An adaptive synthetic control chart for detecting shifts in the process mean. *J Korean Soc Qual Manag.* 2004;32(4):169-183.
35. Song S-I, Park H-K. Development of VSI synthetic control chart. *J Korean Soc Qual Manag.* 2005;33(1):1-10.
36. Lee LY, Khoo MBC, Teh SY, Lee MH. A variable sampling interval synthetic X chart for the process mean. *PLoS ONE.* 2015;10(5): e0126331.
<https://doi.org/10.1371/journal.pone.0126331>
37. Lee J-W, Lim T-J. A VSSI-CRL synthetic control chart. *J Korean Oper Res Manag Sci Soc.* 2005;30(4):1-14.
38. Yu S, Wan Q, Wei Z, Tang T. Statistical design of an adaptive synthetic X control chart with run rule on service and management operation. *Sci Program.* 2016;2016:1-7.
<https://doi.org/10.1155/2016/9629170>
39. Costa AFB, Machado MAG. A side-sensitive synthetic chart combined with a VSS X chart. *Comput Ind Eng.* 2016;91:205-214.
40. Hu XL, Castagliola P, Sun J, Khoo MBC. The effect of measurement errors on the synthetic X chart. *Qual Reliab Eng Int.* 2015;31(8):1769-1778.
41. Haq A, Khoo MBC. A new synthetic control chart for monitoring process mean using auxiliary information. *J Stat Comput Simul.* 2016;86(15):3068-3092.
42. Haq A. New synthetic CUSUM and synthetic EWMA control charts for monitoring the process mean using auxiliary information. *Qual Reliab Eng Int.* 2017;33(7):1549-1565.
43. Hu XL, Sun J. Synthetic X chart for AR(1) autocorrelated processes. Proceedings of the 27th Chinese Control and Decision Conference (CCDC), 2015 (pp. 7–12). DOI:
<https://doi.org/10.1109/CCDC.201527161658>.
44. Muttlak H, Al-Sabah W. Statistical quality control based on ranked set sampling. *J Appl Stat.*

2003;30(9):1055-1078.

45. Haq A, Brown J, Moltchanova E. New synthetic control charts for monitoring process mean and process dispersion. *Qual Reliab Eng Int.* 2015;31(8):1305-1325.
46. Haq A, Brown J, Moltchanova E. New synthetic EWMA and synthetic CUSUM control charts for monitoring process mean. *Qual Reliab Eng Int.* 2016;32(1):269-290.
47. Chen FL, Huang HJ. A synthetic control chart for monitoring process dispersion with sample range. *Int J Adv Manuf Technol.* 2005;26(7-8):842-851.
48. Huang HJ, Chen FL. A synthetic control chart for monitoring process dispersion with sample standard deviation. *Comput Ind Eng.* 2005;49(2):221-240.
49. Rajmanya SV, Ghute VB. The synthetic D chart under non-normality. *Int J Eng Res Technol.* 2013;2(4):2002-2010.
50. Rajmanya SV, Ghute VB. A synthetic control chart for monitoring process variability. *Qual Reliab Eng Int.* 2014;30(8):1301-1309.
51. Guo B, Wang BX, Cheng Y. Optimal design of a synthetic chart for monitoring process dispersion with unknown in-control variance. *Comput Ind Eng.* 2015;88:78-87.
52. Lee MH, Khoo MBC. Synthetic double sampling S chart. *Commun Stat Theory Methods.* 2017;46(12):5914-5931.
53. Haq A, Brown J, Moltchanova E. A new synthetic exponentially weighted moving average control chart for monitoring process dispersion. *Qual Reliab Eng Int.* 2016;32(1):241-256.
54. Calzada ME, Scariano SM. A synthetic control chart for the coefficient of variation. *J Stat Comput Simul.* 2013;83(5):853-867.
55. Tran KP, Nguyen HD, Nguyen QT, Chattinnawat W. One-sided synthetic control charts for monitoring the coefficient of variation with measurement errors. Proceedings of the 2018 IEEE International Conference on Industrial Engineering and Engineering Management (IEEM 2018) Bangkok, Thailand
56. Costa AFB, Rahim MA. A synthetic control chart for monitoring the process mean and variance. *J Qual Maint Eng.* 2006;12(1):81-88.
57. Chen FL, Huang HJ. Variable sampling interval synthetic control charts for jointly monitoring process mean and standard deviation. *Int J Ind Eng Theory Appl Prac.* 2006;13(2):136-146.
58. Costa AFB, de Magalhães MS, Epprecht EK. Monitoring the process mean and variance using a synthetic control chart with two-stage testing. *Int J Prod Res.* 2009;47(18):5067-5086.
59. Lee MH, Khoo MBC. The synthetic mean square error control chart. *Commun Stat Simul Comput.* 2014;43(6):1523-1542.
60. Scariano SM, Calzada ME. A note on the lower-sided synthetic chart for exponentials. *Qual Eng.* 2003;15(4):677-680.

61. Cheng Y, Sun L, Guo B. Phase II synthetic exponential charts and effect of parameter estimation. *Qual Technol Quan Manag.* 2018;15(1):125-142.
62. Sun L, Wang BX, Guo B, Xie M. Synthetic exponential control charts with unknown parameter. *Commun Stat Simul Comput.* 2018;47(8):2360-2377.
63. Yeong WC, Khoo MBC, Wu Z, Castagliola P. Economically optimum design of a synthetic \bar{X} chart. *Qual Reliab Eng Int.* 2012;28(7):725-741.
64. Chung K-J. A simplified procedure for the economic design of \bar{X} -charts. *Int J Prod Res.* 1990;28(7):1239-1246.
65. Yeong WC, Lim SL, Chong ZL, Ng PS. A cost comparison of the synthetic and Shewhart \bar{X} charts. Proceedings of the 4th World Congress on Mechanical, Chemical and Material Engineering, Spain: Madrid, 2018; DOI: <https://doi.org/10.11159/icmie18.130> (pp. 1-8).
66. Yeong WC, Khoo, MBC. Sensitivity analyses of the design parameters of the economically optimal synthetic chart. Proceedings of the 3rd International Conference on Management, Economics and Social Sciences, Kuala Lumpur: Malaysia 2013 (pp. 122–124).
67. Yeong WC, Khoo, MBC, Lee MH, Rahim MA. Economic and economic statistical designs of the synthetic \bar{X} chart using loss functions. *Eur J Oper Res* 2013; 228(3):571–581.
68. Yeong WC, Khoo MBC, Ou Y, Castagliola P. Economic-statistical design of the synthetic \bar{X} chart with estimated process parameters. *Qual Reliab Eng Int.* 2014;31(5):863-876.
69. Lee MH, Khoo MBC. The economic and economic statistical designs of the synthetic double sampling \bar{X} chart. *Commun Stat Simul Comput.* 2018;1-20.
<https://doi.org/10.1080/03610918.2018.1455869>
70. Aghaulor CD, Ezekwem C. An economic design of a modified synthetic double sampling control chart for process monitoring. *Int J Eng Res Technol.* 2016;5(11):445-460.
71. Hu XL, Castagliola P, Sun JS, Khoo MBC. Economic design of the upper-sided synthetic S^2 chart with measurement errors. *Int J Prod Res.* 2016;54(19):5651-5670.
72. Lee MH, Khoo MBC. Economic-statistical design of synthetic max chart. *Qual Technol Quan Manag.* 2018;15(3):301-327.
73. Wan Q, Wu Y, Zhou W, Chen X. Economic design of an integrated adaptive synthetic \bar{X} chart and maintenance management system. *Commun Stat Theory Methods.* 2018;47(11):2625-2642.
74. Wu Z, Yeo SH, Spedding TA. A synthetic control chart for detecting fraction nonconforming increases. *J Qual Technol.* 2001;33(1):104-111.
75. Bourke PD. Performance comparisons for the synthetic control chart for detecting increases in fraction nonconforming. *J Qual Technol.* 2008;40(4):461-475.
76. Haridy S, Wu Z, Khoo MBC, Yu F-J. A combined synthetic and np scheme for detecting increases in fraction nonconforming. *Comput Ind Eng.* 2012;62(4):979-988.
77. Castagliola P, Wu S, Khoo MBC, Chakraborti S. Synthetic phase II Shewhart-type attributes

- control charts when process parameters are estimated. *Qual Reliab Eng Int.* 2014;30(3):315-335.
78. Lee MH, Khoo MBC. Optimal design of synthetic np control chart based on median run length. *Commun Stat Theory Methods.* 2017;46(17):8544-8556.
 79. Chong ZL, Khoo MBC, Castagliola P. Synthetic double sampling np control chart for attributes. *Comput Ind Eng.* 2014;75(1):157-169.
 80. Adnaik SB, Gadre MP. Modified synthetic control chart for one-step Markov-dependent processes. *Commun Stat Theory Methods.* 2015;44(5):942-952.
 81. Ghute VB, Shirke DT. A multivariate synthetic control chart for monitoring process mean vector. *Commun Stat Theory Methods.* 2008;37(13):2136-2148.
 82. Aparisi F, de Luna MA. The design and performance of the multivariate synthetic- T^2 control chart. *Commun Stat Theory Methods.* 2009;38(2):173-192.
 83. Khoo MBC, Atta AMA, Wu Z. A multivariate synthetic control chart for monitoring the process mean vector of skewed populations using weighted standard deviations. *Commun Stat Simul Comput.* 2009;38(7):1493-1518.
 84. Khoo MBC, Wong VH, Wu Z, Castagliola P. Optimal designs of the multivariate synthetic chart for monitoring the process mean vector based on the median run length. *Qual Reliab Eng Int.* 2011;27(8):981-997.
 85. Khoo MBC, Wu Z, Castagliola P, Lee HC. A multivariate synthetic double sampling T^2 control chart. *Comput Ind Eng.* 2013;64(1):179-189.
 86. Yeong WC, Khoo MBC, Lee MH, Rahim MA. Economically optimal design of a multivariate synthetic T^2 chart. *Commun Stat Simul Comput.* 2014;43(6):1333-1361.
 87. Simões FD, Leoni RC, Machado MAG, Costa AFB. Synthetic charts to control bivariate processes with autocorrelated data. *Comput Ind Eng.* 2016;97:15-25.
 88. Costa AFB, Machado MAG. Synthetic control charts with two stage sampling for monitoring bivariate processes. *Pesquisa Oper.* 2007;27(1):117-130.
 89. Dargopatil P, Ghute V. New sampling strategies to reduce the effect of autocorrelation on the synthetic T^2 chart to monitor bivariate process. *Qual Reliab Eng Int.* 2018;35(1):30-46.
<https://doi.org/10.1002/qre.2378>
 90. Celano G, Castagliola P. A synthetic control chart for monitoring the ratio of two normal variables. *Qual Reliab Eng Int.* 2016;32(2):681-696.
 91. Machado MAG, Costa AFB, Rahim MA. The synthetic control chart based on two sample variances for monitoring the covariance matrix. *Qual Reliab Eng Int.* 2009;25(5):595-606.
 92. Ghute VB, Shirke DT. A multivariate synthetic control chart for process dispersion. *Qual Technol Quan Manag.* 2008;5(3):271-288.
 93. Lee MH, Khoo MBC. Multivariate synthetic |S| control chart with variable sampling interval. *Commun Stat Simul Comput.* 2015;44(4):924-942.

94. Lee MH, Khoo MBC. Combined synthetic and $|S|$ chart for monitoring process dispersion. *Commun Stat Simul Comput.* 2017;46(7):5698-5711.
95. Lee MH, Khoo MBC. Optimal designs of multivariate synthetic $|S|$ control chart based on median run length. *Commun Stat Theory Methods.* 2017;46(6):3034-3053.
96. Ghute VB, Shirke DT. Joint monitoring of multivariate process using synthetic control charts. *Int J Stat Manag Syst.* 2007;1(1–2):129-141.
97. Liu L, Zhong JL, Ma YZ. A multivariate synthetic control chart for monitoring covariance matrix based on conditional entropy. In: Qi E, Shen J, Dou R, eds. *Proceedings of the 19th International Conference on Industrial Engineering and Engineering Management.* Berlin, Heidelberg: Springer-Verlag; 2013:99-107.
98. Guerrero-Cusumano J-L. Testing variability in multivariate quality control: a conditional entropy measure approach. *Inf Sci.* 1995;86(1–3):179-202.
99. Lee MH. The design of the multivariate synthetic exponentially weighted moving average control chart. *Commun Stat Simul Comput.* 2012;41(10):1785-1793.
100. Lee MH, Khoo MBC, Xie M. An optimal control procedure based on multivariate synthetic cumulative sum. *Qual Reliab Eng Int.* 2014;30(7):1049-1058.
101. Haridy S, Wu Z, Abhary K, Castagliola P, Shamsuzzaman M. Development of a multiattribute synthetic- np chart. *J Stat Comput Simul.* 2014;84(9):1884-1903.
102. Khoo MBC, Castagliola P, Liew JY, Teoh WL, Maravelakis PE. A study on EWMA charts with runs-rules—the Markov chain approach. *Commun Stat Theory Methods.* 2016;45(14):4156-4180.
103. Chakraborti S, Graham MA. Nonparametric (distribution-free) control charts: an updated overview and some results. *Qual Eng.* 2018. *Accepted.*
<https://doi.org/10.1080/08982112.2018.1549330>
104. Gadre MP, Rattihalli RN. A group run control chart for detecting shifts in the process mean. *Econ Qual Contr.* 2004;19:29-43.
105. Saha S, Khoo MBC, Lee MH, Castagliola P. A side-sensitive modified group runs double sampling (SSMGRDS) control chart for detecting mean shifts. *Commun Stat Simul Comput.* 2018;47(5):1353-1369.